JOURNAL OF SOLID STATE CHEMISTRY **124,** 77–82 (1996)
ARTICLE NO. 0210

Charge Compensation in Gd-Doped $CaTiO_3$

E. R. Vance,[1] R. A. Day, Z. Zhang, B. D. Begg, C. J. Ball, and M. G. Blackford

Advanced Materials Program, ANSTO, Menai, New South Wales 2234, Australia

Received October 16, 1995; in revised form February 29, 1996; accepted March 5, 1996

$Ca_{(1-x)}Gd_{(x)}TiO_3$ samples prepared by sintering in air at 1550°C exhibit a primary perovskite-structured solid solution for x up to about 0.2. It is concluded from quantitative X-ray microanalysis using a scanning electron microscope that charge compensation in these solid solutions takes place via the formation of one formula unit of Ti^{3+} per formula unit of Gd. High-resolution transmission electron microscopy showed that the $x = 0.15$ sample consisted of a pure perovskite structure, with no observable stacking faults and only a few dislocations. Microanalysis showed that Gd^{3+} substituted for Ca^{2+} can be charge compensated by Al^{3+} substituted for Ti^{4+}, as expected. Microanalysis also indicated that charge compensation can take place in air-fired $Ca_{(1-3x/2)}Gd_{(x)}TiO_3$ by $x/2$ formula units of Ca vacancies per formula unit of Gd for compositions in which $x <$ 0.3.

INTRODUCTION

Larson *et al.* (1) have studied Gd-doped perovskite of nominal composition $Ca_{0.925}Gd_{0.075}TiO_3$, fired in air at 1400°C. They found from electron paramagnetic resonance that Gd^{3+} was incorporated on the Ca^{2+} site, as would be expected from the similarity of ionic sizes of Ca^{2+} and Gd^{3+}. The X-ray structure was found to be very similar to that of undoped perovskite, and they argued that charge compensation for the aliovalent Gd^{3+} ions arose via Ca and/or Ti vacancies.

While the ABO_3 perovskite structure is well known for its ability to accommodate A-site vacancies, cation vacancies are still costly in terms of free energy relative to aliovalent charge compensators. Reduction of Ti^{4+} to Ti^{3+} would allow vacancy-free charge compensation, so although Larson *et al.* (1) rejected this mechanism we decided to seek further evidence.

If charge compensation occurs by vacancies on a single set of sites, the formula would be of the form $Ca_{(1-3x/2)}Gd_{(x)}[\ ]_{(x/2)}TiO_3$ or $Ca_{(1-x)}Gd_{(x)}[\ ]_{(x/4)}Ti_{(1-x/4)}O_3$, depending on whether the cation vacancy [ ] was a Ca or Ti species, respectively. The (Ca + Gd)/Ti ratios would then be $(1 - x/2)$ or $(1 - x/4)^{-1}$, rather than unity (which would be the value if charge compensation occurred by reduction of Ti^{4+} to Ti^{3+}), so precise chemical analysis of the Gd-doped perovskite should enable us to distinguish between these models. We have prepared samples of composition $Ca_{(1-x)}Gd_{(x)}TiO_3$, which would be expected to be single phase if charge compensation occurs by reduction of Ti^{4+} to Ti^{3+}. A further series of samples of composition $Ca_{(1-3x/2)}Gd_{(x)}TiO_3$, which would be single phase if compensation occurs by Ca vacancies, was also prepared. The compositions of individual grains in these samples were determined by analytical electron microscopy. Measurements were also made on further samples, of composition $Ca_{(1-x)}Gd_{(x)}Ti_{(1-x)}Al_{(x)}O_3$, where the ratio (Ca + Gd)/(Ti + Al) should be unity.

The crystallinity of samples of nominal $Ca_{0.85}Gd_{0.15}TiO_3$ and $Ca_{0.85}Gd_{0.10}TiO_3$ stoichiometry was checked using transmission electron microscopy. We have also measured the density and unit cell parameters of the $Ca_{0.85}Gd_{0.15}TiO_3$ sample, which should indicate, in principle, if there are vacancies on both the Ca and Ti sites, and, having concluded from the microanalysis studies that Ti^{3+} was the charge compensator for Gd, have made efforts to detect Ti^{3+} in this sample directly by a variety of techniques.

EXPERIMENTAL

Samples of nominal composition $Ca_{(1-x)}Gd_{(x)}TiO_3$ (x = 0.0–0.5), $Ca_{(1-3x/2)}Gd_{(x)}\ TiO_3$ (x = 0.0–0.3), and $Ca_{(1-x)}Gd_{(x)}Ti_{(1-x)}Al_{(x)}O_3$ (x = 0.0–0.8) were made by the oxide route, in which the relevant oxides and carbonates were used as the starting materials, with the desired reaction taking place during sintering of cold-pressed, calcined material. Pellets were sintered at 1300°C for 2 h, reground and pressed, and refired for 1 week at 1550°C. All heating was performed in an air atmosphere.

Polished sections of epoxy-impregnated pellets were examined with a JEOL JSM-6400 scanning electron microscope (SEM). The perovskite crystals in the sintered samples were well-formed, with grain sizes ~20–50 μm. Quantitative analyses of individual grains were performed

[1] To whom correspondence should be addressed.

0022-4596/96 $18.00

using a Tracor Northern MICRO-ZII energy-dispersive X-ray detector and Series II TN5502 analyzer attached to the SEM. An accelerating voltage of 15 kV and a constantly monitored beam current kept at 1 nA were used. The analyzer was calibrated using TiO_2, Al_2O_3, CaF_2, and Gd metal as standards, and the calibration was checked using pure $CaTiO_3$ and $Gd_2Ti_2O_7$ as reference materials during analysis of the Gd-doped perovskites. The standards and the full range of compositions from all three sets of perovskites were mounted in a single epoxy block, carbon coated, and analyzed in a single combined calibration and analytical session. Acquisition live times of 500 s were used on the standards and perovskites in order to achieve a high degree of analytical precision for preparations containing only small amounts of Gd. In a bid to also ensure accuracy, five sets of 500 s X-ray spectra were obtained from each standard during calibration, and these were combined and averaged for use as reference spectra. The X-ray spectra were processed on-line using the Tracor Northern MICROQ analytical software and PRZ matrix correction procedure. The output consists of nonnormalized weight percentage analyses of individual cations and oxygen.

High-resolution transmission electron microscopy and selected area diffraction were performed with a JEOL 2000FX transmission electron microscope, using small fragments of perovskite mounted on a holey carbon film. Powder X-ray diffraction was carried out with a Siemens D500 diffractometer, using Co$K\alpha$ radiation. Density measurements were made by helium gas pycnometry with a Quantrachrome Multipycnometer on samples which were finely powdered (<38 μm), to avoid errors due to closed pores. Calibration measurements were made on Si powder and undoped perovskite, $CaTiO_3$.

X-ray photoelectron spectroscopy (XPS) was carried out in ultrahigh vacuum ($<1 \times 10^{-9}$ Torr) with a Kratos XSAM 800 pci system. The main analysis chamber is attached to a preparation chamber where samples can be fractured *in situ* ($\sim 1 \times 10^{-7}$ Torr). The Ti 2p XPS spectra were measured using a Mg$K\alpha$ X-ray source (1253.6 eV) operated at 15 kV and 15 mA. The analyzed sample area was approximately 0.2 mm^2. The spectrometer pass energy was set to 20 eV to provide adequate resolution. In order to correct for the energy shift caused by steady-state charging, the electron binding energies (E_B) were calibrated against the Ti $2p_{3/2}$ emission at $E_B = 458.8$ eV (4). Linear backgrounds were subtracted from the XPS spectra. Sintered samples of $CaTiO_3$ and $Ca_{0.85}Gd_{0.15}TiO_3$ were cleaned ultrasonically in acetone and methanol before measurements. The Ti 2p XPS spectra of both as-sintered (i.e., in its air-exposed state) and fractured Gd-doped surfaces were measured, and the as-sintered $CaTiO_3$ surface was measured to serve as a standard.

X-ray absorption spectra near the Ti K edge were measured on ~0.1 mm thick powder samples of TiO_2, Ti_2O_3, $CaTiO_3$, and $Ca_{0.85}Gd_{0.15}TiO_3$ at the Australian National Beamline Facility on the Photon Factory synchrotron located at Tsukuba, Japan. Cathodoluminescence spectra were recorded on a system composed of a JEOL 35C scanning electron microscope fitted with an Oxford Instruments cathodoluminescence attachment.

RESULTS

Composition

The X-ray results showed that the solid solution limit of Gd in air-fired $Ca_{(1-x)}Gd_{(x)}TiO_3$ perovskite preparations is given by $x \sim 0.2$; pyrochlore-structured $Gd_2Ti_2O_7$ appeared as the second phase at higher values of x. SEM showed that in samples with $x \geq 0.25$ the composition of the perovskite phase was substantially constant at about $Ca_{0.81}Gd_{0.19}TiO_3$. However, in a sample with $x = 0.2$ the composition of the perovskite phase was $\sim Ca_{0.83}Gd_{0.17}TiO_3$, with a corresponding amount of $Gd_2Ti_2O_7$. The reason for the smaller amount of Gd in the perovskite in this specimen is not known.

In some samples with $x < 0.15$, SEM revealed the presence of Gd_2TiO_5, Gd_2O_3, and TiO_2 in addition to the perovskite, but the amounts were only quite small (<1% abundance). The overall perovskite stoichiometry was in good agreement with the starting composition, but there was some variation in composition of individual grains from the mean, with x varying from the nominal composition by up to 20%. However, for all grains examined the composition was of the form $Ca_{(1-x)}Gd_{(x)}TiO_3$ (Fig. 1). This strongly suggests that, in this series of air-fired specimens, the charge compensation mechanism for x formula units

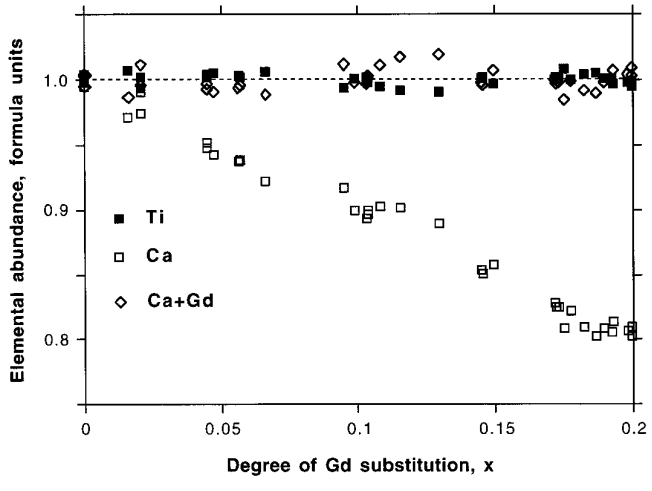

FIG. 1. Compositions of perovskite grains in the $Ca_{(1-x)}Gd_{(x)}TiO_3$ series. The ordinate gives the number of atoms of Ca, (Ca + Gd), and Ti per formula unit of perovskite.

of Gd^{3+} is partial replacement of Ti^{4+} by x formula units of Ti^{3+}.

The $Ca_{(1-3x/2)}Gd_{(x)}TiO_3$ samples were essentially single-phase perovskite for $x < 0.3$ but became two-phase with the development of pyrochlore for $x > 0.3$. Detailed analysis by SEM of the compositions of individual perovskite grains (Fig. 2) showed that they corresponded to those expected for Ca vacancies. The compositions were very close to the starting compositions for $x < 0.3$. For $x \geq 0.3$ the perovskite composition remained at $x = 0.29$.

The Al-containing samples gave perovskite compositions in good agreement with the nominal composition, $Ca_{(1-x)}Gd_{(x)}Ti_{(1-x)}Al_{(x)}O_3$, i.e., the numbers of formula units of Gd and Al were always equal (Fig. 3) even though the compositions of individual grains varied somewhat from the average value. Thus we conclude that, as expected, the Al in the Ti site compensates Gd in the Ca site via $Ca^{2+} + Ti^{4+} \leftrightarrow Gd^{3+} + Al^{3+}$.

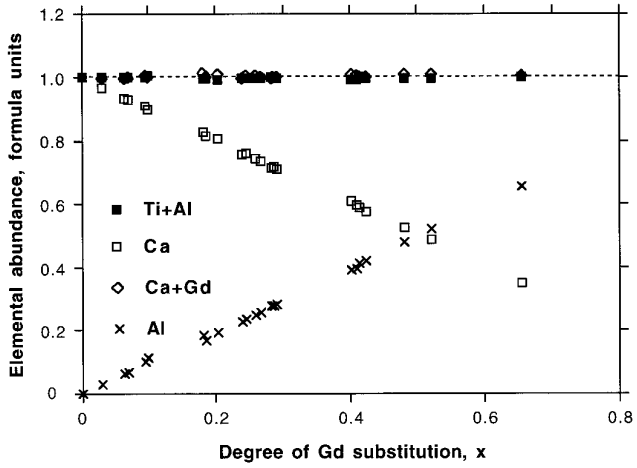

FIG. 3. Compositions of perovskite grains in the $Ca_{(1-x)}Gd_{(x)}Ti_{(1-x)}Al_{(x)}O_3$ series. The ordinate gives the number of atoms of Ca, (Ca + Gd), Al, and (Al + Ti) per formula unit of perovskite.

Unit Cell Parameters

Measurements of unit cell parameters of a number of Gd-doped perovskites are shown in Table 1. There is a small but significant increase in unit cell volume in the $Ca_{(1-x)}Gd_{(x)}TiO_3$ series with increasing x. The radius of Gd^{3+} is less than that of Ca^{2+} (by about 0.06 Å, Shannon (2)), so substitution of Gd^{3+} for Ca^{2+} would be expected to lead to a decrease in unit cell volume. However, the ionic radius of Ti^{3+} is larger than that of Ti^{4+} (again by about 0.06 Å (2)), and this may explain why the unit cells of the $Ca_{(1-x)}Gd_{(x)}TiO_3$ samples are larger than that of $CaTiO_3$. The cell volume of $Ca_{0.55}Gd_{0.3}TiO_3$ was less than that of $CaTiO_3$, by ~0.1%. This is a smaller decrease than would be expected from the substitution of 0.3 formula units of Gd^{3+} for the same amount of Ca^{2+}, so presumably Ca vacancies partially compensate the effect of Gd substitution. Qualitatively, the parameter decrease in the Al-containing samples is expected, since Al^{3+} is a substantially smaller ion than either Ti^{4+} or Ti^{3+}.

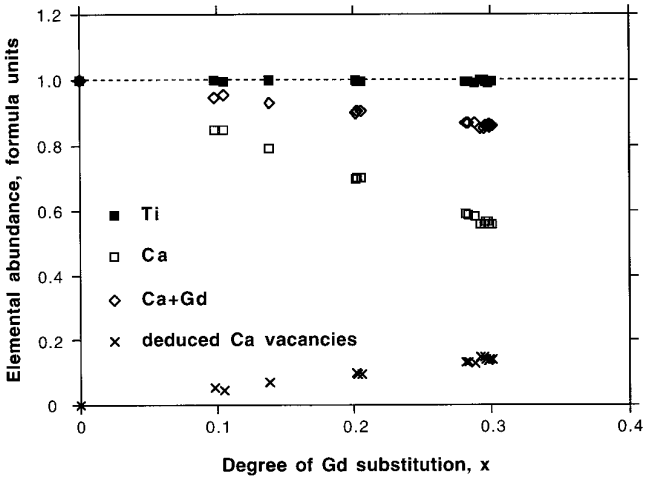

FIG. 2. Compositions of perovskite grains in the $Ca_{(1-3x/2)}Gd_{(x)}TiO_3$ series. The ordinate gives the number of atoms of Ca, (Ca + Gd), and Ti per formula unit of perovskite.

TEM Studies

The only lattice defects observed in high-resolution transmission electron micrographs of the $Ca_{0.85}Gd_{0.15}TiO_3$ sample were the occasional dislocation, and no evidence of superstructures was observed in the diffraction pattern. This shows that the structure of the sample is the basic perovskite structure, which is consistent with the idea that charge compensation of Gd takes place by reduction of Ti^{4+} to Ti^{3+}. Also there was no evidence for stacking faults or microscopic deviation from the perovskite structure in high-resolution micrographs of $Ca_{0.85}Gd_{0.1}TiO_3$, so the Ca

TABLE 1
Unit Cell Parameters of Some Gd-Substituted Perovskites

Composition	a (Å)	b (Å)	c (Å)	V (Å^3)
$CaTiO_3$[a]	5.4405_2	7.6436_5	5.3812_3	223.8
$Ca_{0.925}Gd_{0.075}TiO_3$[b]	5.449_1	7.647_1	5.381_1	224.2
$Ca_{0.85}Gd_{0.15}TiO_3$	5.4530_4	7.6504_5	5.3853_5	224.7
$Ca_{0.55}Gd_{0.3}TiO_3$	5.442_1	7.642_1	5.377_1	223.6
$Ca_{0.75}Gd_{0.25}Ti_{0.75}Al_{0.25}O_3$	5.410_2	7.609_2	5.353_2	220.3
$Ca_{0.5}Gd_{0.5}Ti_{0.5}Al_{0.5}O_3$	5.372_2	7.561_2	5.324_2	216.2

[a] Ref. (12).
[b] Ref. (1).

vacancies deduced to be present in this composition are evidently randomly distributed, and not condensed in the form of ordered vacancy-containing structures.

XPS

The Ti 2*p* XPS spectrum of the $CaTiO_3$ surface confirmed that only Ti^{4+} cations are present, as shown by the Ti^{4+} $2p_{3/2}$ and $2p_{1/2}$ peaks in Fig. 4a. The spin-orbit splitting is 5.7 eV, which is consistent with the results obtained from a stoichiometric TiO_2 {110} surface (3). The full width half maxima (FWHM) of the Ti^{4+} $2p_{3/2}$ and $2p_{1/2}$ peaks are 1.36 and 1.97 eV, respectively, determined by fitting the spectra with two 50% Gaussian/50% Lorentzian curves. The intensity ratio $I(2p_{3/2})/I(2p_{1/2})$ was constrained at 2, as given by the ratio of the occupation numbers of the subshell state $(2j + 1)$. The spectrum of the fractured $Ca_{0.85}Gd_{0.15}TiO_3$ surface shows the presence of a small amount of Ti^{3+}, as indicated by the small shoulder on the lower binding energy side of the Ti^{4+} $2p_{3/2}$ XPS peak (Fig. 4b). In order to determine the Ti^{3+}/Ti^{4+} ratio, the same curve fitting procedure was used.

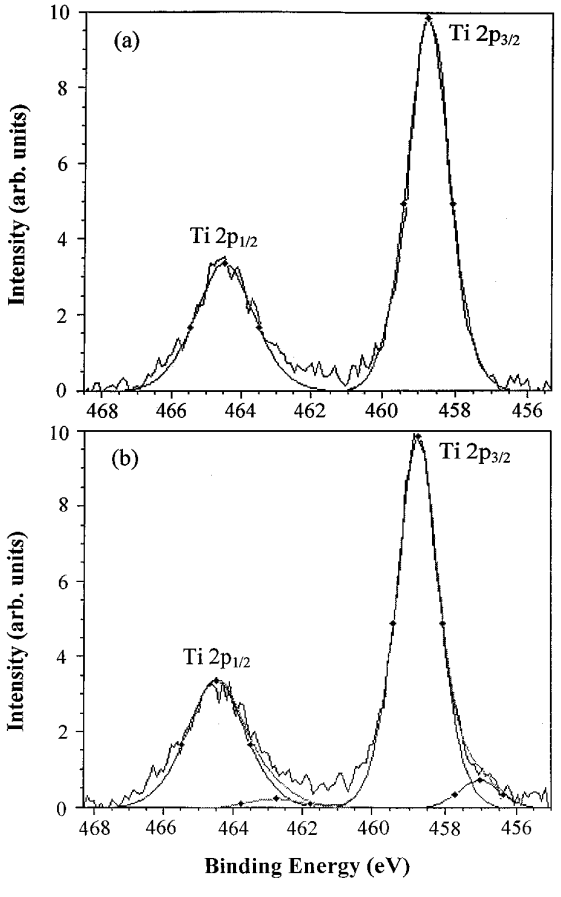

FIG. 4. XPS spectra from (a) $CaTiO_3$ and (b) $Ca_{0.85}Gd_{0.15}TiO_3$.

To ensure the validity of the curve fitting, several constraints were imposed: (i) the fitting parameters from the $CaTiO_3$ Ti 2*p* XPS spectrum were used to fit the Ti^{4+} peaks; (ii) the Ti^{3+} peak positions were fixed at 1.7 eV lower binding energy than those of the Ti^{4+} peaks (4); (iii) the intensity ratio $I(Ti^{3+}\ 2p_{3/2})/I(Ti^{3+}\ 2p_{1/2})$ was also constrained at 2; and (iv) the FWHM of the Ti^{3+} peaks were taken to be equal to those of the corresponding Ti^{4+} peaks. From the curve fitting results, the Ti^{3+}/Ti^{4+} ratio in $Ca_{0.85}Gd_{0.15}TiO_3$ was found to be approximately 8%.

The Ti 2*p* XPS spectrum of as-sintered $Ca_{0.85}Gd_{0.15}TiO_3$ did not show a shoulder on the lower binding energy side of the Ti^{4+} $2p_{3/2}$ XPS peak. This suggests that the concentration of Ti^{3+} in the surface of this sample was negligible. The difference between the as-sintered and fractured surfaces might arise from adsorbed species on the as-sintered surface, e.g., O_2^-, O_2^{2-}, O^-, and O^{2-}. During the adsorption process electrons could be transferred from the surface Ti^{3+} ions to the adsorbed species, resulting in the absence of Ti^{3+} in the surface region. For the surface fractured *in situ* much less adsorption could occur, due to the high-vacuum environment, and therefore a fractured surface should be a better representative of the bulk than an as-sintered surface. Finally it should be borne in mind that some limited adsorption can occur even under high-vacuum conditions, which may be why the experimentally determined Ti^{3+}/Ti^{4+} ratio (~8%) was less than the ~18% predicted for $Ca_{0.85}Gd_{0.15}TiO_3$.

Other Evidence for Ti^{3+} in $Ca_{0.85}Gd_{0.15}TiO_3$

Other attempts to confirm the presence of Ti^{3+} were inconclusive. X-ray absorption near-edge spectroscopy (XANES) using synchrotron radiation may give a shift of a few electron-volts for Ti^{3+} relative to Ti^{4+} (5), but the absorption edges themselves are strongly affected by pre-edge phenomena arising from octahedral site distortion, making it very difficult to identify a small fraction of Ti^{3+} in a majority of Ti^{4+}. The Ti K edge absorption spectra of $CaTiO_3$ and $Ca_{0.85}Gd_{0.15}TiO_3$ are shown in Fig. 5, together with a spectrum from Ti_2O_3. Although it is difficult to draw definite conclusions, the arrowed feature near the bottom of the Ti edge for the Gd-doped sample, i.e., within the energy interval of 4.988–4.992 keV, may indicate the presence of some Ti^{3+}, since this kind of feature is observed for Ti_2O_3 but not for TiO_2 (5) or $CaTiO_3$. Also, the general slight shift to lower energy of the absorption edge as a whole for $Ca_{0.85}Gd_{0.15}TiO_3$ relative to $CaTiO_3$ may reflect the presence of Ti^{3+}. The results for TiO_2 (not shown in Fig. 5) and Ti_2O_3 were in good agreement with data published previously (5).

Cathodoluminescence of the Gd–perovskite ($x = 0.15$)

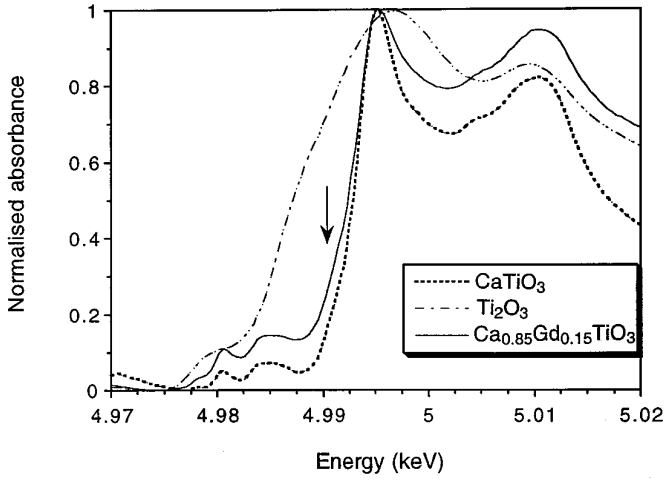

FIG. 5. XANES spectra from $CaTiO_3$, $Ca_{0.85}Gd_{0.15}TiO_3$, and Ti_2O_3.

yielded no evidence of Ti^{3+}, which would have been expected in the vicinity of 750–850 nm (6), but this is not conclusive since no evidence of Ti^{3+} was seen from cathodoluminescence in the titanate phases of a Synroc (7) sample either (8), and these certainly contain some Ti^{3+} because Synroc is fabricated under very reducing conditions (7).

Density measurements were also inconclusive, because we were unable to measure the composition sufficiently accurately. The calculated density differences between Ti^{3+}- and vacancy-compensated preparations with $x = 0.15$ are only ~1%, and a change in x of ~0.015 would produce a similar change in density. As noted earlier, SEM showed that the compositions of individual grains frequently differed from the nominal composition, and from each other, by more than this value.

A referee has pointed out that if the samples could be dissolved, redox titration could be employed to verify the presence of Ti^{3+}. However no significant dissolution was observed even when the samples were finely powdered and boiled for long periods in (nonoxidizing) HCl. Of course this was not surprising since perovskite is known to be very chemically durable, which is why it is a key phase in Synroc (7).

DISCUSSION

Larson *et al.* (1) considered charge compensation by reduction of Ti^{4+} to be unlikely mainly because of lack of significant color in the highly doped samples. However, although compounds containing Ti^{3+} might be expected to produce a violet/black color due to single-ion d–d transitions, which can give rise to a broad absorption band centered at 500 nm (9), Prewitt *et al.* (10) have reported a Ti^{3+}-bearing clinopyroxene, $NaTiSi_2O_6$, as having only a light-green color, and following the work of Bunker (11) we have prepared a ceramic containing a substantial proportion of a Cs analog of this compound that was white in color. It follows that absence of strong violet/black coloration in Gd-bearing perovskites should not be taken as conclusive evidence against a Ti^{3+} mechanism of charge compensation. However the question of color remains unresolved.

Within the framework of an ionic model for perovskite, the microanalysis measurements on $Ca_{(1-x)}Gd_{(x)}TiO_3$ perovskite samples fired in air provide strong evidence that charge compensation in these materials occurs by reduction of Ti^{4+} to Ti^{3+}, and this is partly confirmed by the XPS observations. Though at first sight the existence of Ti^{3+} seems incompatible with a firing atmosphere of air, crystal-chemical stabilization forces provide a mechanism: a good example is the well-known existence in an air atmosphere of $CePO_4$ (Ce^{3+}) and CeO_2 (Ce^{4+}). In the present work it appears that in Ca-deficient conditions charge compensation occurs through Ca vacancies. This may explain the smaller range of compositions within the nominal $Ca_{0.7}Gd_{0.2}TiO_3$ sample than of the Ti^{3+}- and Al^{3+}-compensated preparations; cation diffusion would be expected to be faster in samples with a high concentration of vacancies.

Charge compensation for Gd substituted for Ca is also possible in principle through the formation of oxygen interstitials, but this seems unlikely since the close-packed nature of the perovskite structure would not seem to have room for significant populations of such interstitials. Also, the presence of interstitial oxygen would reduce the measured amounts of Ca, Ti, and Gd present and result, contrary to experiment, in analytical totals expressed as weight percentages of CaO, TiO_2 (here all Ti would be tetravalent), and Gd_2O_3 systematically adding to less than 100%. Generally the analytical totals fall within the range of 99.5 to 100.5% in all members of the three compositional series examined. For a perovskite of composition $Ca_{0.8}Gd_{0.2}TiO_3$ the totals expressed as weight percentage oxides would be expected to lie around 99.0% due to ~2 At% of interstitial oxygen, not 100%.

We conclude that charge compensation in air-fired Gd-substituted perovskites occurs by reduction of Ti^{4+} to Ti^{3+} and/or by Ca vacancies, depending on the (Ca + Gd)/Ti ratio in the starting materials.

ACKNOWLEDGMENTS

We thank G. J. Thorogood for performing the cathodoluminescence measurements and R. W. Cheary for use of the facilities in the Department of Applied Physics, UTS. We also thank G. P. Eller for discussions, G. Foran, D. Cookson, and R. Garrett for assistance in the operation of the

Australian National Beamline Facility at the Photon Factory, Tsukuba, and the referees for helpful comments.

REFERENCES

1. E. M. Larson, P. G. Eller, J. D. Purson, C. F. Pace, M. P. Eastman, R. B. Greegor, and F. W. Lytle, *J. Solid State Chem.* **73,** 480 (1988).
2. R. D. Shannon, *Acta Crystallogr. A***32,** 751 (1976).
3. Z. Zhang, Ph.D. Thesis, Yale University (unpublished), 1993.
4. S. O. Saied, J. L. Sullivan, T. Choudhury, and C. G. Pearce, *Vacuum* **38,** 917 (1988).
5. G. J. McCarthy, W. B. White, and R. Roy, *Mater. Res. Bull.* **4,** 251 (1969).
6. R. C. Powell, G. E. Venikouas, L. Xi, and J. K. Tyminski, *J. Chem. Phys.* **84,** 662 (1986).
7. A. E. Ringwood, S. E. Kesson, K. D. Reeve. D. M. Levins, and E. J. Ramm, *in* ''Radioactive Waste Forms for the Future'' (W. Lutze and R. C. Ewing, Eds.), p. 233. Elsevier, Amsterdam, Netherlands, 1988.
8. G. J. Thorogood, M.Sc. Thesis, University of Technology, Sydney (unpublished), 1995.
9. D. S. McClure, *J. Chem. Phys.* **36,** 2757 (1972).
10. C. T. Prewitt, R. D. Shannon, and W. B. White, *Contrib. Mineral. Petrol.* **35,** 77 (1972).
11. B. D. Bunker, Oral presentation at TWRS/TDPO Mid-Year Program Review, Richland, WA, May 16–20, 1994.
12. H. E. Swanson, H. F. McMurdie, M. C. Morris, E. H. Evans, and B. Paretzkin, *NBS Monogr. U.S.* **25,** Section 9 (1971).